Manuscript Details

Manuscript number	EFA_2018_1355_R1
Title	Experimental measurement of temperature-dependent equivalent stress-strain curves of a 420 MPa structural steel with axisymmetric notched tensile specimens
Article type	Research Paper

Abstract

Recently, the authors in this paper proposed a correction function to determine material's equivalent stress-strain curve with axisymmetric-notched tensile specimens. In this study, tensile tests were performed at room temperature, -30°C and -60°C with axisymmetric notched tensile specimens to verify this method and to identify the equivalent stress-strain curves of a 420 MPa structural steel. A high-speed camera was used together with the so-called edge-tracing method to calculate average true strain. The material's equivalent stress-strain curve was also measured with extensometer and smooth round bar specimens. Experimental results show that equivalent stress-strain curve of this structural steel is sensitive to test temperature. Equivalent stress-stress curves obtained from axisymmetric notched tensile specimens by using the proposed correction function show good agreement with those from extensometer before diffuse necking and from Bridgman correction at large strain using smooth tensile specimens. Since fracture strain strongly depends on the notch geometry, it is recommended to use axisymmetric notched tensile specimens with smaller when applying the proposed correction function to measure material's equivalent stress-strain curve.

Keywords	equivalent stress-strain curve; low temperature; axisymmetric notched tensile specimen; Bridgman correction; large strain.

Corresponding Author	zhiliang zhang
Corresponding Author's Institution	Norwegian University of Science and Technology
Order of Authors	Shengwen Tu, Xiaobo Ren, Jianying He, zhiliang zhang
Suggested reviewers	Erling Østby, Jian Shuai, Jacques Besson, Aleksandar Sedmak

Submission Files Included in this PDF

File Name [File Type]

Cover letter.docx [Cover Letter]

Detailed response to the reviewers comments.docx [Response to Reviewers]

Response to the first reviewer's comments.pdf [Review Reports]

Highlight.pdf [Highlights]

revised manuscript.docx [Manuscript File]

Highlights

- A newly proposed correction function for deriving equivalent stress-strain curve with axisymmetric notched tensile specimens was verified experimentally.
- Significant temperature effect on the equivalent stress-strain curves was observed.
- Results obtained with the proposed correction method show good agreement with the well-known Bridgman correction at large strain.

Experimental measurement of temperature-dependent equivalent stress-strain curves of a 420 MPa structural steel with axisymmetric notched tensile specimens

Shengwen Tu[1], Xiaobo Ren[2], Jianying He[1], Zhiliang Zhang[1,*]

[1]Department of Structural Engineering, Norwegian University of Science and Technology, Trondheim 7491, Norway

[2]SINTEF Industry, Trondheim 7465, Norway

Highlights

- A newly proposed correction function for deriving equivalent stress-strain curve with axisymmetric notched tensile specimens was verified experimentally.
- Significant temperature effect on the equivalent stress-strain curves was observed.
- Results obtained with the proposed correction method show good agreement with the well-known Bridgman correction at large strain.

* Corresponding author: Tel: +47 73592530
E-mail address: zhiliang.zhang@ntnu.no (Z. Zhang)
Fax: +47 73594700

Nomenclature

a	current minimum cross-section radius
a_0	initial minimum cross-section radius
A	current minimum cross-section area
d_0	specimen outer diameter
E	Young's modulus
H	material zone height in the notch
P	tensile load
R	current notch curvature radius
R_0	initial notch curvature radius
a/R	current notch radius ratio
a_0/R_0	initial notch radius ratio
T	stress triaxiality
ε	average true strain
ε'	engineering strain
$\varepsilon_{P_{\max}}$	strain at the maximum load
ξ	correction factor for axisymmetric notched tensile specimen
ξ_B	Bridgman correction factor
σ_0	yield stress
σ'	engineering stress
σ_{eq}	von Mises equivalent stress
σ_T	true stress

Experimental measurement of temperature-dependent equivalent stress-strain curves of a 420 MPa structural steel with axisymmetric notched tensile specimens

Shengwen Tu[1], Xiaobo Ren[2], Jianying He[1], Zhiliang Zhang [1]

[1]Department of Structural Engineering, Norwegian University of Science and Technology, Trondheim 7491, Norway

[2]SINTEF Industry, Trondheim 7465, Norway

Abstract

Recently, we proposed a correction function to determine material's equivalent stress-strain curve with axisymmetric-notched tensile specimens. In this study, we performed tensile tests at room temperature, -30℃ and -60℃ with axisymmetric notched tensile specimens to verify this method and to identify the equivalent stress-strain curves of a 420 MPa structural steel. A high-speed camera was used together with the so-called edge-tracing method to calculate average true strain. We also measured the material's equivalent stress-strain curve with extensometer and smooth round bar specimens. Experimental results show that equivalent stress-strain curve of this structural steel is sensitive to test temperature. Equivalent stress-stress curves obtained from axisymmetric notched tensile specimens by using the proposed correction function show good agreement with those from extensometer before diffuse necking and from Bridgman correction at large strain using smooth tensile specimens. Since fracture strain strongly depends on the notch geometry, it is recommended to use axisymmetric notched tensile specimens with smaller a_0/R_0 when applying the proposed correction function to measure material's equivalent stress-strain curve.

Keywords: *equivalent stress-strain curve; low temperature; axisymmetric notched tensile specimen; Bridgman correction; large strain.*

1. Introduction

Identifying material's equivalent stress-strain curve in large strain is very important for large deformation analysis, such as plastic forming [1, 2], ductile fracture analysis with finite element method [3-8]. Usually, we use smooth round bar specimen [9, 10] or smooth specimen with rectangular cross-section [11-13] to measure material's equivalent stress-strain curve with extensometer. The limitation of such method is that only the data before diffuse necking can be used directly. There are several methods to determine material's true stress-strain curve in large range of strain. For thick materials, smooth round bar specimen can be used when the instantaneous minimum cross-section area is measured. The strain ε is then characterized by the specimen minimum cross-section area reduction:

$\varepsilon = 2\ln(a_0/a)$. a_0 and a are the specimen initial and current minimum cross-section radius, respectively. The true stress or axial average stress σ_T is calculated by dividing the load P by the instantaneous minimum cross-section area. For very thin plate material, Zhang [14] proposed a method to calculate the post-necking minimum cross-section area of rectangular cross-section specimens, as a function of specimen thickness reduction. With Zhang's method, true stress-strain curves from flat tensile specimens can be obtained at large strain. It should be noted that after diffuse necking, tri-axial stress state occurs in the necked region. The true stress differs with von Mises equivalent stress σ_{eq} [9, 15] and should be corrected. Fig. 1 schematically presents the difference of the true stress and von Mises equivalent stress after diffuse necking.

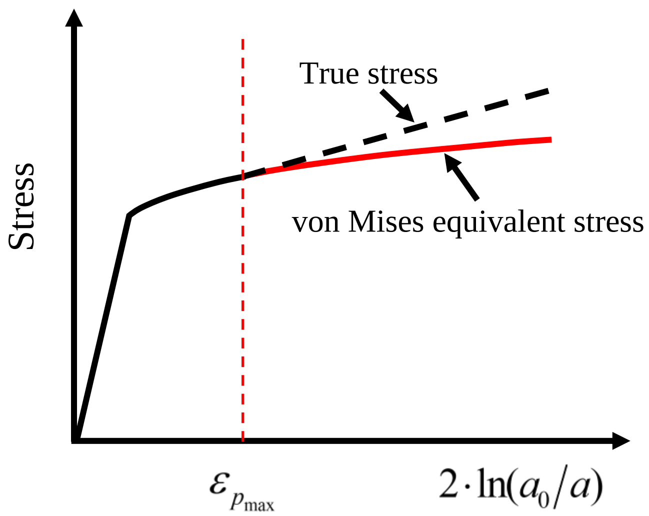

Fig. 1 Illustration of the difference between true stress and von Mises equivalent stress for tensile test with smooth round bar specimen after diffuse necking ($\varepsilon > \varepsilon_{P_{\max}}$).

Diffuse necking occurs after the maximum tensile load, hence the true stress should be corrected when the strain is larger than the strain corresponding to the maximum tensile load, $\varepsilon_{P_{\max}}$. Bridgman [9] performed analytical analysis with necked round bar specimen and proposed a correction factor ξ_B:

$$\begin{aligned} &\xi_B = (1+2R/a)\cdot\ln(1+a/2R) \\ &\sigma_{eq} = \sigma_T/\xi_B \end{aligned} \tag{1}$$

where R is the neck curvature radius. By dividing the true stress in Fig.1 by ξ_B, the material's equivalent stress can be calculated. Indeed, R is very difficult to measure accurately. Le Roy [16] proposed an empirical formula to calculate the notch curvature radius ratio a/R:

$$a/R = 1.1\cdot(\varepsilon - \varepsilon_{P_{\max}}) \tag{2}$$

Combined with Eq. (1) – (2), true stress-strain curve from a smooth round bar specimen can be converted to material's equivalent stress-strain curve after diffuse necking. The Bridgman correction factor ξ_B

works well at strain slightly larger than $\varepsilon_{P_{\max}}$. As the strain further increases, errors between the material's equivalent stress and the Bridgman corrected equivalent stress occurs and increases with the increase of strain [15]. The errors range from several percentages to more than 10% [15, 17]. Recent numerical analyses [18-20] show that the stress distribution at the necked specimen minimum cross-section differs significantly with Bridgman's analytical solution. These errors are mainly attributed to the assumption that the equivalent strain is uniform in the specimen minimum cross-section. Similar to the Bridgman method, several other correction methods have been proposed [21]. The main difference of these methods is the determination of the curvature radius of the longitudinal stress trajectories. Though the Bridgman correction method is not very accurate when the strain is large, it still can be used as reference. Ling [22] proposed a so-called weighted average method to measure the true stress-strain curve from rectangular cross-section specimen, by setting the power law hardening as lower bound and the linear hardening as the upper bound for the equivalent stress. The correction proposed by Ling is a kind of hybrid experimental-numerical modeling method and the determination of the weight constant is time consuming. Scheider [23] proposed a correction factor as a function of strain and $\varepsilon_{P_{\max}}$ to derive equivalent stress-strain curve with flat tensile specimen. However, Scheider's method can only be used for specimens with the aspect ratio of 1:4. Choung [24, 25] also proposed a method to measure equivalent stress-strain curves with flat tensile specimens. The minimum cross-section area should be measured manually with digital calipers and a micrometer. It is worth noting that both Shceider [23] and Choung's [24, 25] method are based on inverse numerical analyses.

To measure the true stress-strain curve of each individual material zone in a weldment, Zhang [26] proposed a correction function, with which the true stress-strain curve from an axisymmetric notched tensile specimen can be converted to the corresponding one from a smooth round bar specimen. This method is not accurate at large strain, but lay a foundation for our recent work [27, 28]. With further numerical studies, we identified a 'magic' axisymmetric notched tensile specimen [28]. With only one single correction factor, true stress-strain curve from the 'magic' notched specimen can be converted to material's equivalent stress-strain curve in a large range of strain accurately, and no Bridgman correction is needed. The limitation is that failure strain of this 'magic' notched specimen can be much smaller than that from a smooth round bar specimen, sometimes.

Recently, we found a new correction function to determine material's equivalent stress-strain with 'any' axisymmetric notched tensile specimens [27]. The correction function can be used to the perfectly plastic material and hardening material, and also to weldments. In this study, we performed tensile tests at room temperature, -30 ℃ and -60 ℃ with axisymmetric notched tensile specimens machined from a 420 MPa structural steel plates to verify the proposed correction method. The correction function is introduced in detail in section 2. The experimental procedure is presented in section 3. We also measured the material's equivalent stress-strain curve with extensometer and smooth round bar specimens. Before diffuse necking, the equivalent stress-strain curves from axisymmetric notched tensile specimens are compared with those from extensometer. With Eq. (1)-(2), we also performed Bridgman correction with smooth round bar specimen to obtain reference equivalent stress-strain curves after diffuse necking. Results and discussions are presented in section 4. The equivalent stress-strain curves are then verified by numerical analyses in section 5. Main conclusions are presented in section 6.

2. Axisymmetric notched tensile specimen method

Axisymmetric notched tensile specimen has been widely applied in characterizing material's mechanical properties [29-31]. For inhomogeneous material, such as weldment, it is impossible to measure the equivalent stress-strain curve in a targeted material zone with cross-weld smooth round bar specimen or flat tensile specimen, due to the nature of unpredictable fracture position. By introducing an axisymmetric notch on the smooth round bar specimen, the deformation is restrained mainly in the notched region under uniaxial tensile loading [26-28]. Fig. 2 (a) schematically shows the geometry information of the axisymmetric notched tensile specimen. Similar with smooth round bar specimen, the strain is defined by the minimum cross-section area reduction and the true stress is calculated by dividing load by the current minimum cross-section area:

$$\varepsilon = 2 \cdot \ln\left(a_0/a\right) \tag{3}$$

$$\sigma_T = P/\pi a^2 \tag{4}$$

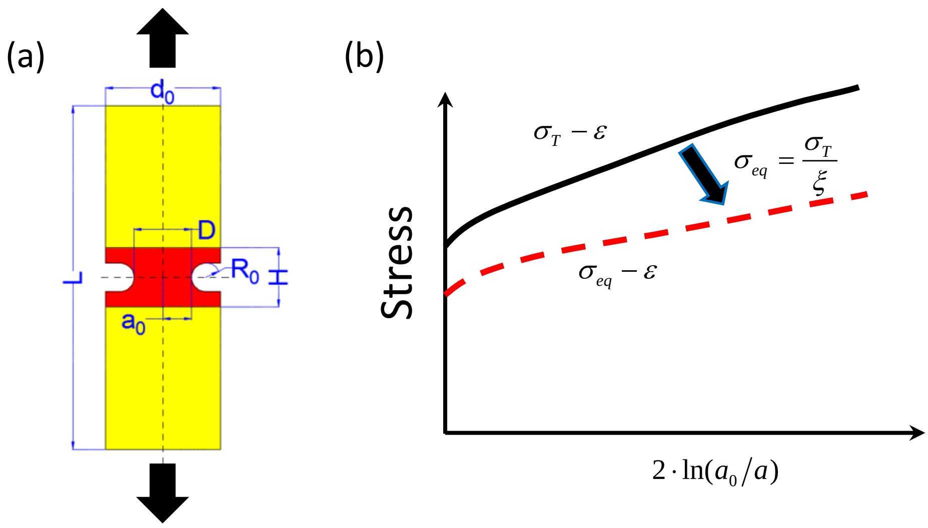

Fig. 2 (a) Geometry of axisymmetric notched tensile specimen. The yellow part can be overmatch, under match or even match with the remain part of the specimen. (b) Conversion of true stress-strain curve from notched specimen to equivalent stress-strain curve by the proposed correction function.

Stress concentration occurs due to the existence of the notch. True stress-strain curve from an axisymmetric notched tensile specimen differs significantly with the material's equivalent stress-strain curve and should be corrected. Our previous study [28] shows that when the specimen geometry requirement $d_0 \geq 3.5a_0$ is fulfilled, true stress-stress curves from axisymmetric notched tensile specimens with the same initial notch radius ratio a_0/R_0 are identical for homogeneous materials. This is true for inhomogeneous material when a_0 is smaller than the material zone length: $a_0 \leq H$.

Recently, we proposed a correction function to convert the true stress-strain curve from any axisymmetric notched tensile specimens to the material's equivalent stress-strain curve [27]. The correction function is written in a general form:

$$\xi = g_{a_0/R_0, n=0}(\varepsilon) \cdot f(\varepsilon_{P_{\max}}) \tag{5}$$

Eq. (5) consists of two parts: the first part describes the notch effect on the true stress-strain curves of the perfectly-plastic material, and displays as a linear function of the true strain ε , Eq. (6). The slope, $b_{1,n=0}$, in Eq. (6) depicts the initial notch geometry effect on the evolution of true stress-strain curve from axisymmetric notched tensile specimen. While the intersection, $b_{2,n=0}$, can be explained as the notch induced stress concentration, sharper notch yields higher stress concentration. The slope and intersection are given in Eq. (7) and Eq. (8) as a function of the initial notch radius ratio, respectively. The second part, as shown in Eq. (9), is a function of $\varepsilon_{P_{\max}}$, describing the effect of strain hardening on the true stress-strain curve of a notched specimen.

$$g_{a_0/R_0, n=0}(\varepsilon) = (b_{1,n=0} \cdot \varepsilon + b_{2,n=0})_{a_0/R_0} \tag{6}$$

$$b_{1,n=0} = 0.03232 \cdot (a_0/R_0)^2 - 0.27 \cdot (a_0/R_0) + 0.3866 \tag{7}$$

$$b_{2,n=0} = -0.04084 \cdot (a_0/R_0)^2 + 0.3557 \cdot (a_0/R_0) + 1.0577 \tag{8}$$

$$f(\varepsilon_{p_{\max}}) = -0.22942 \cdot \varepsilon_{P_{\max}}^2 - 0.36902 \cdot \varepsilon_{P_{\max}} + 1 \tag{9}$$

When ε and $\varepsilon_{P_{\max}}$ are known, the $\sigma_T - \varepsilon$ curve from an axisymmetric notched tensile specimen can be converted to the material's equivalent stress-strain curve by Eq. (10), as demonstrated in Fig. 2 (b). Details about the derivation of this correction function can be referred to ref. [27].

$$\sigma_{eq} = \sigma_T / \xi \tag{10}$$

3. Experiment procedure

To experimentally verify the correction function, we conducted tensile tests with smooth round bar specimens and axisymmetric notched tensile specimens with initial notch radius ratio, a_0/R_0, ranging from 0.5 to 3. The specimens were machined from 50 *mm* thick plates of a 420 MPa steel, along the rolling direction. The specimen configurations are shown in Fig. 3. Our previous numerical studies provide a conservative geometry requirement for axisymmetric notched tensile specimens: $d_0 \geq 3.5a_0$. d_0 is the specimen outer diameter, as seen in Fig. 2. In this study, $a_0 = 6\ mm$ and $d_0 = 20\ mm$. The specimen outer diameter is 1 *mm* smaller than the geometry requirement ($d_0 \geq 3.5a_0$). In order to guarantee that the specimen geometry can be used, we simply performed numerical analysis with power-law hardening material and found that the correction function was still valid.

The tests were carried out at room temperature, -30°C, and -60°C using a universal test machine Instron 5985, with the loading cell of 250 KN. A liquid nitrogen-cooled temperature chamber was used to create low temperature environment. We divided the tests into two packages: in the first package we tested smooth round bar specimens with extensometer at each test temperature, to provide reference equivalent stress-strain curves; in the second package, we used a digital high speed camera to record the specimen deformation for axisymmetric notched tensile specimens, as well as for smooth round bar specimens. The specimen minimum cross-section diameter in the second package was identified with a so-called 'edge-tracing' or 'edge-detection' method [32]. For all the tests, the specimen was loaded in displacement control with the crosshead speed of 0.3 mm/minute.

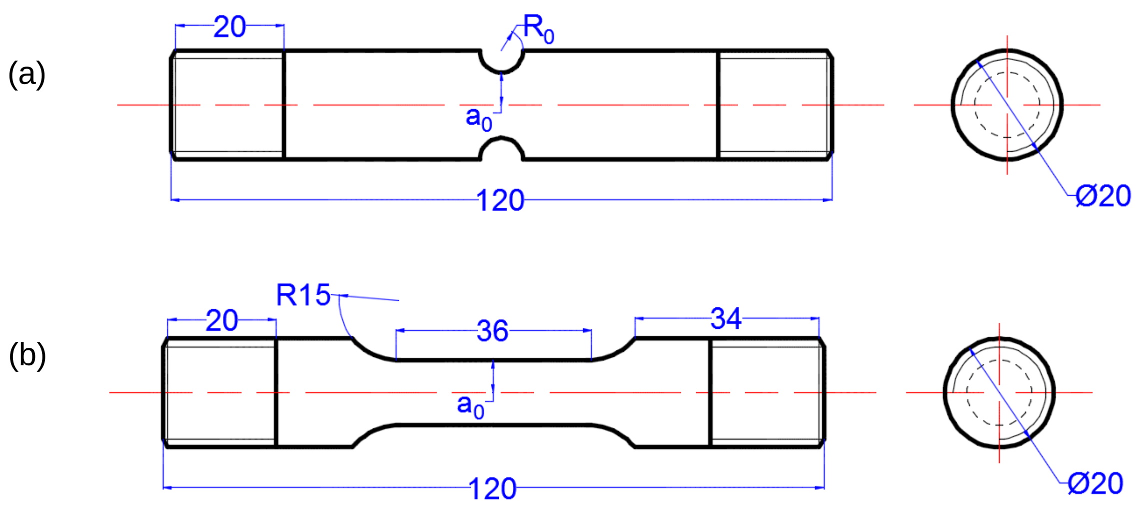

Fig. 3 Sketches of the tensile specimens: (a) axisymmetric notched tensile specimen; (b) smooth round bar specimen.

4. Results and discussion

For the smooth round bar tensile tests with extensometer, the engineering stress σ' is calculated by dividing load by the initial cross-section area ($\sigma' = P/\pi a_0^2$). Engineering strain ε' directly from extensometer and corresponding engineering stress are converted to true strain and true stress by Eq. (11) and Eq. (12):

$$\sigma_T = \sigma'(1+\varepsilon') \tag{11}$$

$$\varepsilon = \ln(1+\varepsilon') \tag{12}$$

Fig. 4 presents the true stress-strain curves at room temperature, -30℃ and -60℃. Obvious temperature effect can be found: true stress-strain curve obtained at lower test temperature presents to be higher. It can also be found that the strain corresponding to the onset of diffuse necking ($\varepsilon_{P_{\max}}$, intersections of the dash lines and the horizontal axis) also increases slightly with decreasing testing temperature. Before diffuse necking, the smooth round bar specimen deforms uniformly, true stress-strain curve also represents material's equivalent stress-strain curve. Therefore, true stress-strain curves in Fig. 4 will be used as reference before diffuse necking in the following discussion.

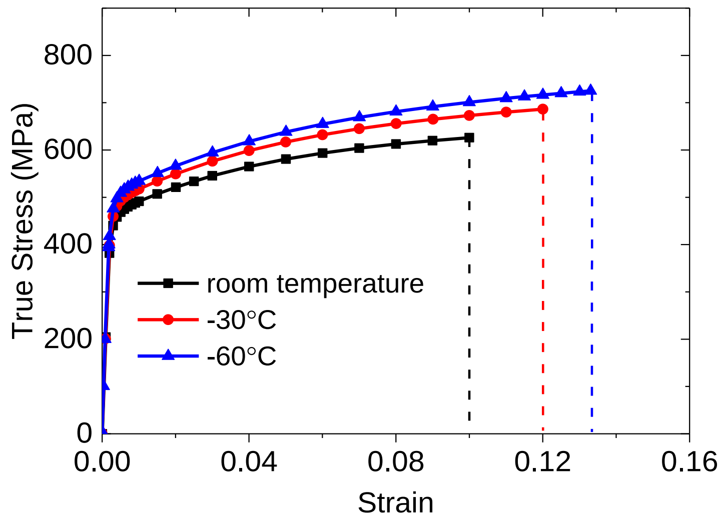

Fig. 4 True stress-strain curves from smooth round bar specimens with extensometer.

For the tensile tests in the second package, the specimen deformation was recorded with a digital high speed camera. The strain for smooth round bar specimens is calculated by Eq. (3), the same for the axisymmetric notched tensile specimens. Engineering stress-strain curves for all the tests in the second package are presented in Fig. 5. As expected, the engineering stress increases with strain firstly; after reaching the maximum value it decreases. Axisymmetric notched tensile specimen with a higher initial notch radius ratio corresponds to a larger peak engineering stress. For example, for the tests performed at room temperature, the maximum engineering stress for specimen with $a_0/R_0 = 0.5$ is 673.55 MPa;

while for specimen with $a_0/R_0 = 3$, the maximum engineering stress is 903.11 MPa. $\varepsilon_{P_{\max}}$ is shown with red dash lines in Fig. 5. It can be seen that $\varepsilon_{P_{\max}}$ for smooth round bar specimen and axisymmetric notched tensile specimens is approximately the same at same testing temperature. This result indicates that for this 420 MPa structural steel, $\varepsilon_{P_{\max}}$ is independent of the specimen notch geometry. It can also be observed that $\varepsilon_{P_{\max}}$ for this material is sensitive to temperature, and it increases slightly with decreasing testing temperatures.

True stress for all the tests in the second package are calculated with Eq. (4). Corresponding true stress-strain curves are presented in Fig. 6. For the smooth round bar specimens in the second package, true stress-strain curve before diffuse necking is exactly the material's equivalent stress-strain curve. After diffuse necking, true stress-strain curves of smooth round bar specimens in Fig. 6 are corrected by Bridgman correction: Eq. (1) and Eq. (2). True stress-strain curves for axisymmetric notched tensile specimens in Fig. 6 are then corrected with Eq. (10). Corresponding equivalent stress-strain curves are presented in Fig. 7, together with the true stress-strain curves with extensometer and equivalent stress-strain curves after performing Bridgman correction with smooth round bar specimens in the second package. Very good agreements can be seen in Fig. 7 between the true stress-strain curves from extensometer and equivalent stress-strain curves corrected by Eq. (10) with axisymmetric notched tensile specimens, at each test temperature. After diffuse necking, equivalent stress-strain curves corrected by Eq. (10) with the axisymmetric notched tensile specimens agree well with the Bridgman corrected equivalent stress-strain curve from smooth round bar specimen, when the strain is smaller than 0.528, 0.699, 0.742 for the tests performed at room temperature, -30°C, and -60°C, respectively. After then, slight difference can be found. The equivalent stress corrected by Eq. (10) is slightly lower than those from the Bridgman correction.

For axisymmetric notched tensile specimen with sharper initial notch (larger a_0/R_0), the specimen failed at smaller strain than that with smaller initial notch radius ratio. For example, for the tests conducted at -30°C, the specimen with $a_0/R_0 = 3$ failed when $\varepsilon = 0.525$; while for the specimen with $a_0/R_0 = 0.5$, it failed at the strain $\varepsilon = 1.14$. This can be explained that the strain at fracture is strongly dependent of stress triaxiality T, which is defined by the ratio of hydrostatic stress and von Mises equivalent stress [33-36]. Fracture strain decreases with the increase of stress triaxiality in the range $T \geq 1/3$. For axisymmetric notched tensile specimen, the stress triaxiality is a function of notch radius ratio and larger than 1/3. Larger a_0/R_0 corresponds to a higher stress triaxiality, therefore, resulting in a smaller failure strain. On the purpose of measuring equivalent stress-strain curve with our correction function in large strain, it is therefore not recommended to use specimens with very larger initial notch radius ratio.

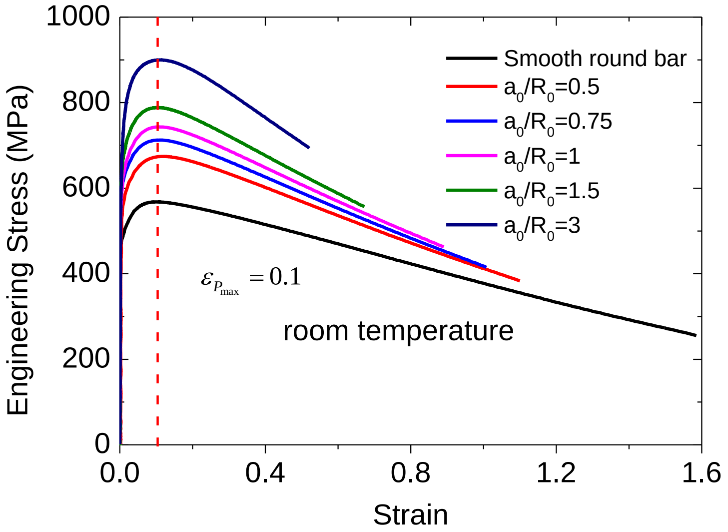

(a)

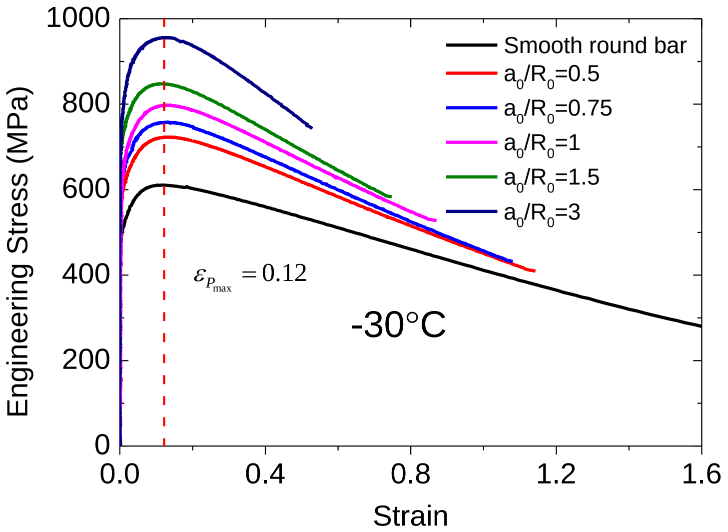

(b)

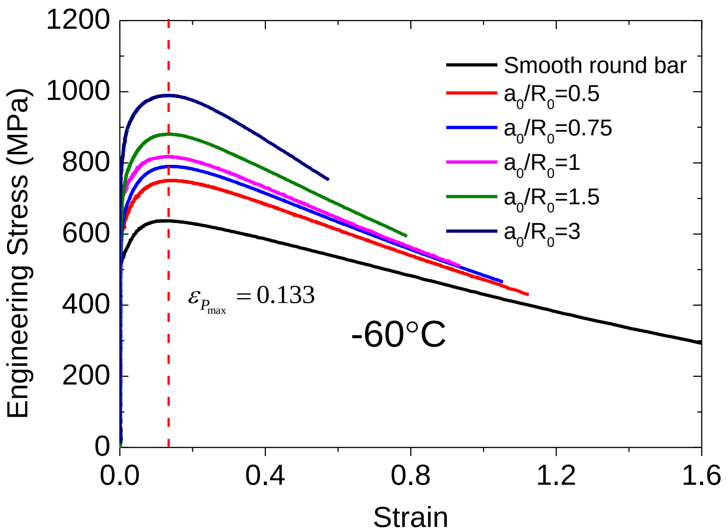

(c)

Fig. 5 Engineering stress-strain curves of smooth round bar and axisymmetric notched tensile specimens: (a) room temperature; (b) -30℃; (c) -60℃. $\varepsilon_{P_{\max}}$ *is also shown with red dash lines.*

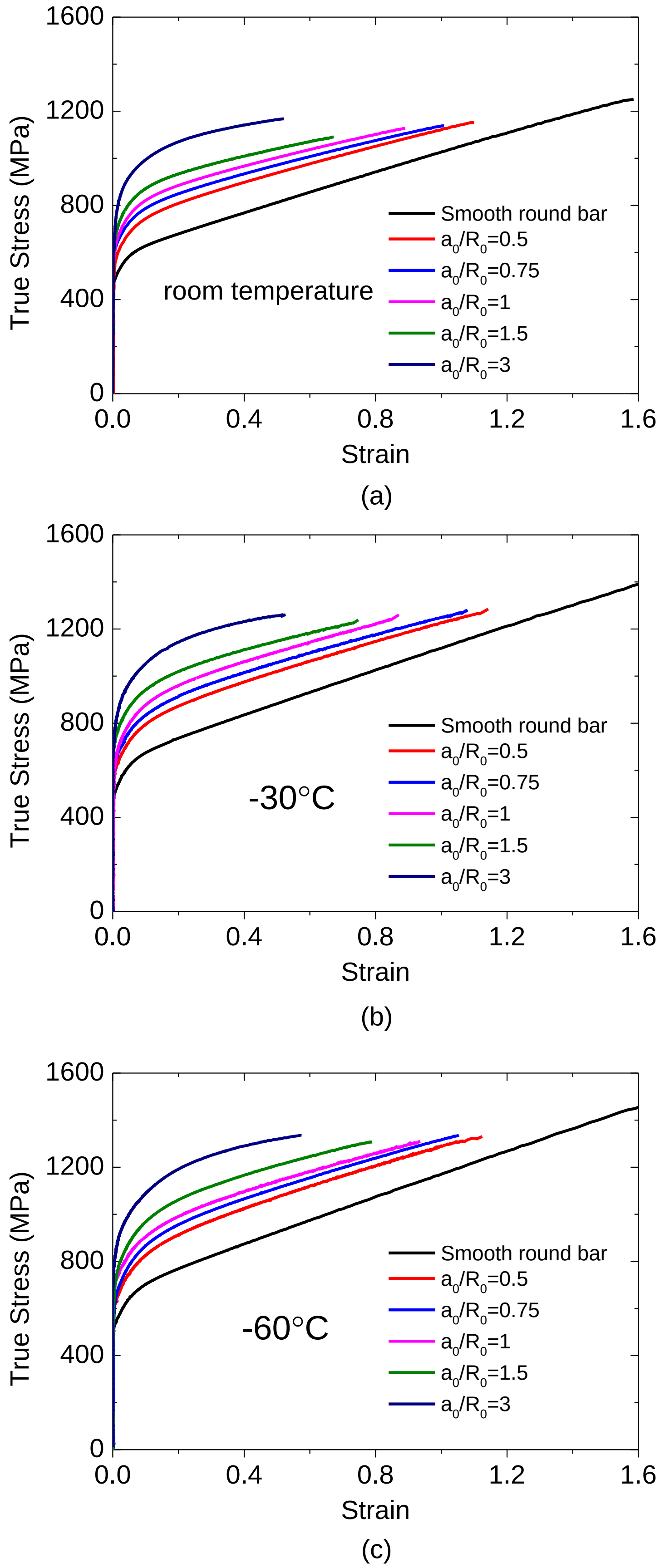

Fig. 6 True stress-strain curves of smooth round bar and axisymmetric notched tensile specimens: (a) room temperature; (b) -30℃; (c) -60℃.

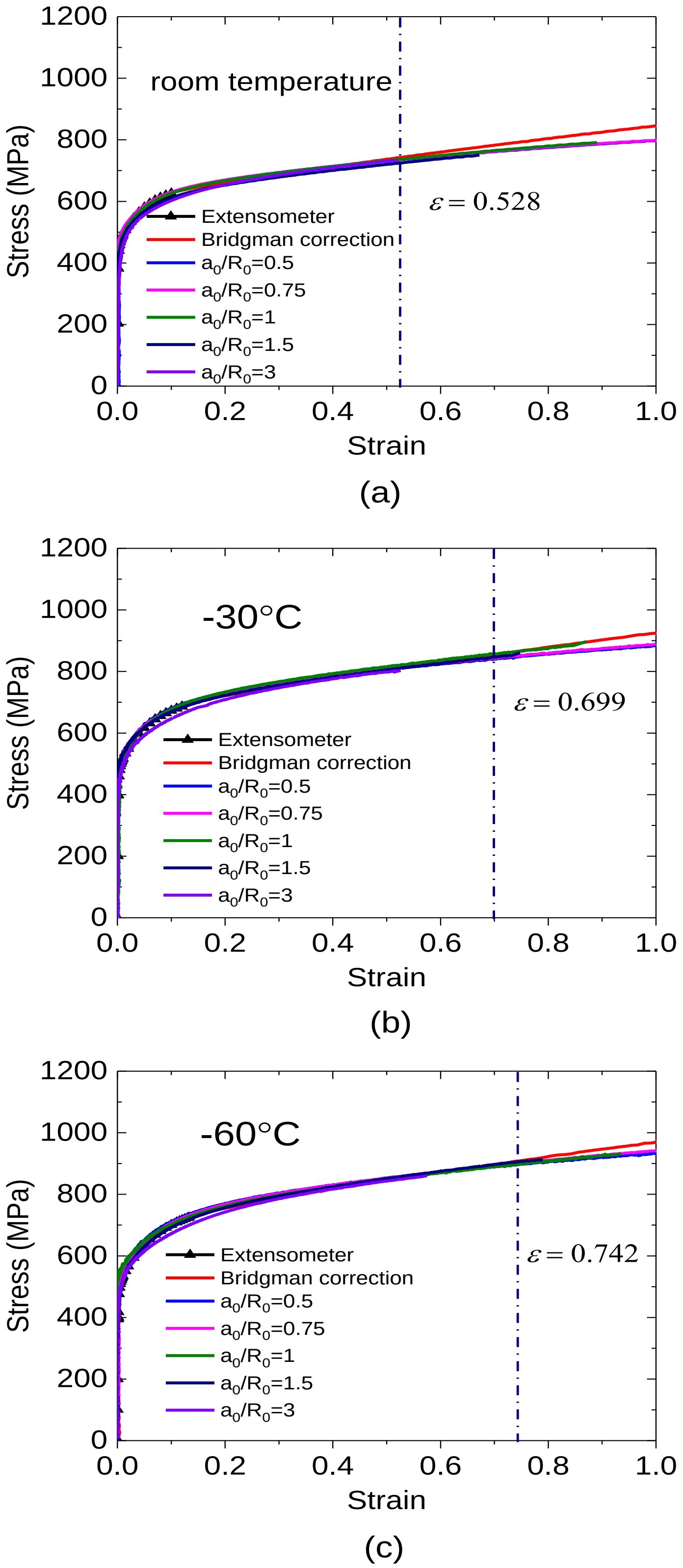

Fig. 7 Equivalent stress-strain curves obtained from axisymmetric notched tensile specimens with the correction function: (a) room temperature; (b) -30℃; (c) -60℃. Equivalent stress-strain curve from smooth round bar specimen from extensometer (before diffuse necking) and from Bridgman correction are also shown for reference.

5. Validation of the equivalent stress-strain curve

The correction method is derived with power-law hardening materials in an inverse manner. Attention should be paid for the application of this correction method, since materials can follow different hardening rules. To guarantee the accuracy of the equivalent stress-strain curve obtained with the correction method, a fast and efficient way is to compare load-strain curves from tests and from numerical analysis, assuming the derived equivalent stress-strain curve as material's equivalent stress-strain curve and used for numerical modeling. Fig. 8 schematically presents the validation procedure. True stress-strain curve from axisymmetric notched tensile specimen in Fig. 8 (a) are corrected with Eq. (10) to obtain the equivalent stress-strain curve in Fig. 8 (b). The equivalent stress-strain curve in Fig. 8 (b) is then used as input stress-strain curve for numerical analysis. Load-strain curves from numerical simulation (see in Fig. 8 (d)) are then compared with those from test, as shown in Fig. 8 (e). When the load-strain curves from test and from numerical simulation show very good agreement, it indicates that the equivalent stress-strain derived with the proposed correction method is accurate.

As an example, equivalent stress-strain curves derived with the axisymmetric notched tensile specimen with $a_0/R_0 = 0.5$ at each test temperature are used for numerical analyses. The geometry used for numerical analyses is the same as in experiments. Numerical anslyses were perforemed with Abaqus/Standard 6.14. Axisymmetric model is used with the 4-noded axisymmetric reduced integration element (CAX4R). The element size is approximately 0.4*0.4 mm in the notch region. Larger deformation is accounted. Symmetric boundary condition is applied in the symmetric plane. The specimen is modelled in displacment control, the same as in the expeirment. Load-strain curves from the experiments and from numerical analyses are presented in Fig. 9.

It can be seen that the load-strain curves from numerical analyses present very good agreement with those from experiments, at each test temperature. It indicates that the deformation on the specimen during loading process can be well captured. It also indicates that the equivalent stress-strain curves derived with the correction function are accurate for this 420 MPa structural steel.

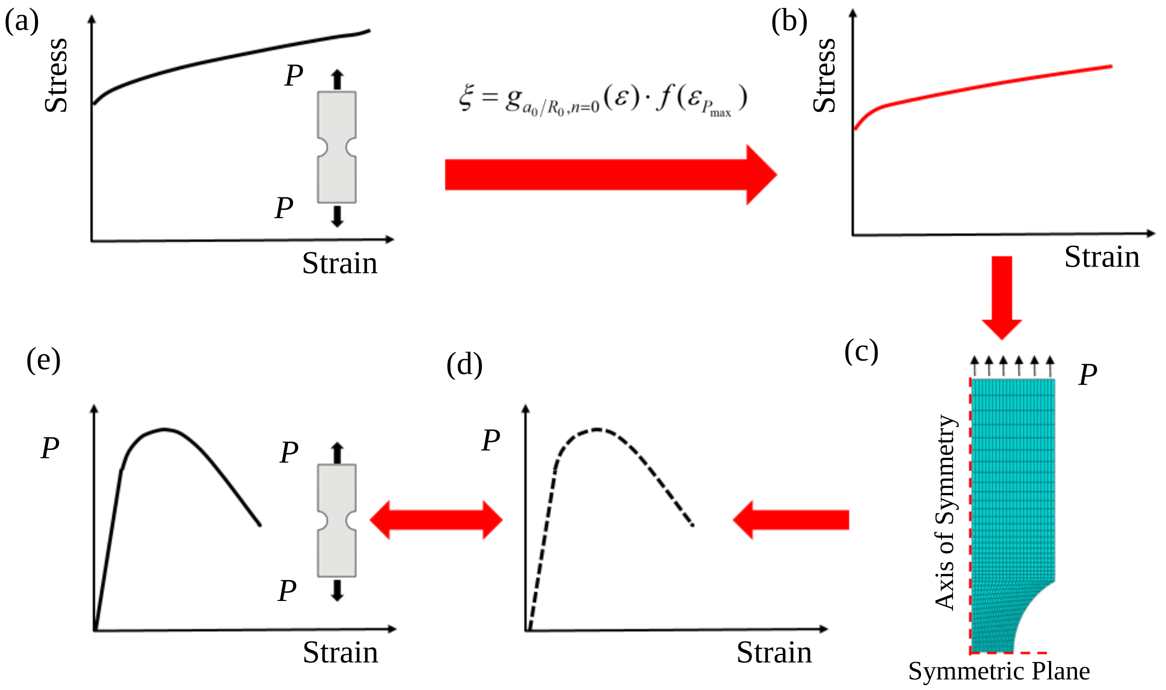

Fig. 8 Procedure for the validation of the equivalent stress-strain curves from axisymmetric notched specimens. (a) true stress-strain curve from axisymmetric notched specimens tensile tests; (b) equivalent stress-strain curve obtained with the proposed correction method; (c) Numerical simulation of tensile tests. (d) Load-strain curves from numerical simulation; (e) Load-strain curves from test.

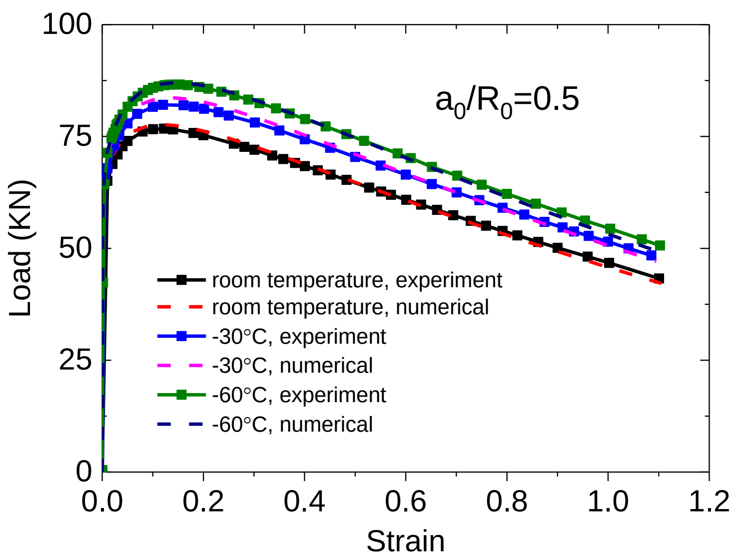

Fig. 9 Comparison of load-strain curves from experiments and from numerical analyses for axisymmetric notched specimen with $a_0/R_0 = 0.5$ *at each test temperature.*

6. Concluding remarks

In this paper, we performed tensile tests with axisymmetric notched tensile specimens with a_0/R_0 ranging from 0.5 to 3 to experimentally verify the recent proposed correction function, by measuring equivalent stress-strain curve of a 420 MPa structural steel at room temperature, -30℃ and -60℃, respectively. Equivalent stress-strain curves by converting true-strain curves from axisymmetric notched tensile specimens with the proposed correction function agree very well with true stress-strain curves from smooth round bar specimen with extensometer together with Bridgman correction. Comparing load-strain curves from the experiments and numerical simulations, it indicates that our correction method works well to explore the material's stress-strain behavior. It is worth noting that the proposed correction function can also be used to measure the equivalent stress-strain curve of each individual material zone in a weldment, by locating the notch in the targeted material zone, once the specimen geometry requirements ($d_0 \geq 3.5a_0$, $a_0 \leq H$) are fulfilled. Due to the stress triaxiality dependence of fracture strain, it is not suggested to use specimens with very sharp notch (large a_0/R_0) to measure material's equivalent stress-strain curve. We recommend to run numerical analysis to verify the equivalent stress-strain curve derived with the correction function to guarantee the validity of test results.

Acknowledgement

The Chinese Scholarship Council is greatly acknowledged for the financial support. The authors wish to thank the Research Council of Norway for funding through the Petromaks 2 Programme, Contract No.228513/E30.

Reference

[1] F.M. Andrade Pires, J.M.A. César de Sá, L. Costa Sousa, R.M. Natal Jorge, Numerical modelling of ductile plastic damage in bulk metal forming, International Journal of Mechanical Sciences 45(2) (2003) 273-294.

[2] O.M. Badr, F. Barlat, B. Rolfe, M.-G. Lee, P. Hodgson, M. Weiss, Constitutive modelling of high strength titanium alloy Ti-6Al-4 V for sheet forming applications at room temperature, International Journal of Solids and Structures 80 (2016) 334-347.

[3] Z.L. Zhang, M. Hauge, C. Thaulow, Two parameter characterization of the near-tip stress field for a bi-material elastic-plastic interface crack, International Journal of Fracture 79 (1996) 65-83.

[4] E. Østby, C. Thaulow, Z.L. Zhang, Numerical simulations of specimen size and mismatch effects in ductile crack growth – Part I: Tearing resistance and crack growth paths, Engineering Fracture Mechanics 74(11) (2007) 1770-1792.

[5] E. Østby, C. Thaulow, Z.L. Zhang, Numerical simulations of specimen size and mismatch effects in ductile crack growth – Part II: Near-tip stress fields, Engineering Fracture Mechanics 74(11) (2007) 1793-1809.

[6] J. Xu, Z.L. Zhang, E. Østby, B. Nyhus, D.B. Sun, Effects of crack depth and specimen size on ductile crack growth of SENT and SENB specimens for fracture mechanics evaluation of pipeline steels, International Journal of Pressure Vessels and Piping 86(12) (2009) 787-797.

[7] J. Xu, Z.L. Zhang, E. Østby, B. Nyhus, D.B. Sun, Constraint effect on the ductile crack growth resistance of circumferentially cracked pipes, Engineering Fracture Mechanics 77(4) (2010) 671-684.

[8] J. Shuai, S. Tu, J. Wang, X. Ren, J. He, Z. Zhang, Determining critical CTOA from energy-load curves with DWTT specimen, Engineering Fracture Mechanics 186 (2017) 47-58.

[9] P.W. Bridgman, Studies in large plastic flow and fracture, MaGraw-Hill, New York, 1952.

[10] D.J. Celentano, Analysis of the Bridgman procedure to characterize the mechanical behavior of materials in the tensile test experiments and simulation, Journal of Applied Mechanics 72 (2005) 149-152.

[11] W.J. Yuan, Z.L. Zhang, Y.J. Su, L.J. Qiao, W.Y. Chu, Influence of specimen thickness with rectangular cross-section on the tensile properties of structural steels, Materials Science and Engineering: A 532 (2012) 601-605.

[12] Z.L. Zhang, J. Ødegård, O.P. Søvik, Determining true stress-strain curve for isotropic and anisotropic materials with rectangular tensile bars: method and verifications, Computational Materials Science 20 (2001) 77-85.

[13] Z.L. Zhang, J. Ødegård, O.P. Søvik, C. Thaulow, A study on determining true stress–strain curve for anisotropic materials with rectangular tensile bars, International Journal of Solids and Structures 38 (2001) 4489-4505.

[14] Z.L. Zhang, M. Hauge, J. Ødegård, C. Thaulow, Determining material true stress-strain curve from tensile specimens with rectangular cross-section, International Journal of Solids and Structures 36 (1999) 3497-3516.

[15] G. La Rosa, G. Mirone, Risitano. A, Postnecking elastoplastic characterization degree of approximation in the bridgman method and properties of the flow stress true stress ratio, Metallurgical and Materials Transactions A 34 (2003) 615-624.

[16] G.L. Roy, J.D. Embury, G. Edward, M.F. Ashby, A model of ductile fracture based on the nucleation and growth of voids, Acta Metallurgica 29 (1981) 1509-1522.

[17] G. Mirone, A new model for the elastoplastic characterization and the stress–strain determination on the necking section of a tensile specimen, International Journal of Solids and Structures 41(13) (2004) 3545-3564.

[18] Y. Bai, X. Teng, T. Wierzbicki, On the Application of Stress triaxiality formula for plane strain fracture testing, Journal of Engineering Material and Technology 131 (2009).

[19] Y. Bao, Dependence of ductile crack formation in tensile tests on stress triaxiality, stress and strain ratios, Engineering Fracture Mechanics 72(4) (2005) 505-522.

[20] Y. Bao, T. Wierzbicki, On the cut-off value of negative triaxiality for fracture, Engineering Fracture Mechanics 72(7) (2005) 1049-1069.

[21] M. Gromada, G. Mishuris, Andreas, Correction formulae for the stress distribution in round tensile specimens at neck presence, Springer2011.

[22] Y. Ling, Uniaxial true stress-strain after necking, AMP Journal of Technology 5 (1996) 37-48.

[23] I. Scheider, W. Brocks, A. Cornec, Procedure for the determination of true stress-strain curves from tensile tests with rectangular cross-section specimens, Journal of Engineering Material and Technology 126 (2004) 70-76.

[24] J. Choung, Comparative studies of fracture models for marine structural steels, Ocean Engineering 36(15-16) (2009) 1164-1174.

[25] J.M. Choung, S.R. Cho, Study on true stress correction from tensile tests, Journal of Mechanical Science and Technology 22(6) (2008) 1039-1051.

[26] Z.L. Zhang, M. Hauge, C. Thaulow, J. Ødegård, A notched cross weld tensile testing method for determining true stress–strain curves for weldments, Engineering Fracture Mechanics 69 (2002) 353-366.

[27] S. Tu, X. Ren, J. He, Z. Zhang, A method for determining material's equivalent stress-strain curve with any axisymmetric notched tensile specimens without Bridgman correction, International Journal of Mechanical Sciences 135 (2018) 656-667.

[28] S. Tu, X. Ren, B. Nyhus, O.M. Akselsen, J. He, Z. Zhang, A special notched tensile specimen to determine the flow stress-strain curve of hardening materials without applying the Bridgman correction, Engineering Fracture Mechanics 179 (2017) 225-239.

[29] N. Noda, Y. Takase, Stress concentration formula useful for all notch shape in a round bar (comparison between torsion, tension and bending), International Journal of Fatigue 28(2) (2006) 151-163.

[30] F. Berto, P. Gallo, P. Lazzarin, High temperature fatigue tests of un-notched and notched specimens made of 40CrMoV13.9 steel, Materials & Design 63 (2014) 609-619.

[31] A. Wormsen, M. Avice, A. Fjeldstad, L. Reinås, K.A. Macdonald, E. Berg, A.D. Muff, Fatigue testing and analysis of notched specimens with typical subsea design features, International Journal of Fatigue 81 (2015) 275-298.

[32] S. Tu, X. Ren, J. He, Z. Zhang, Study of low temperature effect on the fracture locus of a 420 MPa structural steel with the edge tracing method, Fatigue & Fracture of Engineering Materials & Structures On line (2018).

[33] T. Børvik, O.S. Hopperstad, T. Berstad, On the influence of stress triaxiality and strain rate on the behaviour of a structural steel. Part II. Numerical study, European Journal of Mechanics - A/Solids 22(1) (2003) 15-32.

[34] T. Børvik, O.S. Hopperstad, S. Dey, E.V. Pizzinato, M. Langseth, C. Albertini, Strength and ductility of Weldox 460 E steel at high strain rates, elevated temperatures and various stress triaxialities, Engineering Fracture Mechanics 72(7) (2005) 1071-1087.

[35] O.S. Hopperstad, T. Børvik, M. Langseth, K. Labibes, C. Albertini, On the influence of stress triaxiality and strain rate on the behaviour of a structural steel. Part I. Experiments, European Journal of Mechanics - A/Solids 22(1) (2003) 1-13.

[36] Z.L. Zhang, E. NIEMI, Studies on the ductility predictions by different local failure criteria, Engineering Fracture Mechanics 48 (1994) 529-540.

Highlights

- A newly proposed correction function for deriving equivalent stress-strain curve with axisymmetric notched tensile specimens was verified experimentally.
- Significant temperature effect on the equivalent stress-strain curves was observed.
- Results obtained with the proposed correction method show good agreement with the well-known Bridgman correction at large strain.

Experimental measurement of temperature-dependent equivalent stress-strain curves of a 420 MPa structural steel with axisymmetric notched tensile specimens

Shengwen Tu[1], Xiaobo Ren[2], Jianying He[1], Zhiliang Zhang[1,*]

[1]Department of Structural Engineering, Norwegian University of Science and Technology, Trondheim 7491, Norway

[2]SINTEF Industry, Trondheim 7465, Norway

Highlights

- A newly proposed correction function for deriving equivalent stress-strain curve with axisymmetric notched tensile specimens was verified experimentally.
- Significant temperature effect on the equivalent stress-strain curves was observed.
- Results obtained with the proposed correction method show good agreement with the well-known Bridgman correction at large strain.

* Corresponding author: Tel: +47 73592530
E-mail address: zhiliang.zhang@ntnu.no (Z. Zhang)
Fax: +47 73594700

Nomenclature

a	current minimum cross-section radius
a_0	initial minimum cross-section radius
A	current minimum cross-section area
d_0	specimen outer diameter
E	Young's modulus
H	material zone height in the notch
P	tensile load
R	current notch curvature radius
R_0	initial notch curvature radius
a/R	current notch radius ratio
a_0/R_0	initial notch radius ratio
T	stress triaxiality
ε	average true strain
ε'	engineering strain
$\varepsilon_{P_{\max}}$	strain at the maximum load
ξ	correction factor for axisymmetric notched tensile specimen
ξ_B	Bridgman correction factor
σ_0	yield stress
σ'	engineering stress
σ_{eq}	von Mises equivalent stress
σ_T	true stress

Experimental measurement of temperature-dependent equivalent stress-strain curves of a 420 MPa structural steel with axisymmetric notched tensile specimens

Shengwen Tu[1], Xiaobo Ren[2], Jianying He[1], Zhiliang Zhang [1]
[1]Department of Structural Engineering, Norwegian University of Science and Technology, Trondheim 7491, Norway
[2]SINTEF Industry, Trondheim 7465, Norway

Abstract

Recently, the authors in this paper proposed a correction function to determine material's equivalent stress-strain curve with axisymmetric-notched tensile specimens. In this study, tensile tests were performed at room temperature, -30°C and -60°C with axisymmetric notched tensile specimens to verify this method and to identify the equivalent stress-strain curves of a 420 MPa structural steel. A high-speed camera was used together with the so-called edge-tracing method to calculate average true strain. The material's equivalent stress-strain curve was also measured with extensometer and smooth round bar specimens. Experimental results show that equivalent stress-strain curve of this structural steel is sensitive to test temperature. Equivalent stress-stress curves obtained from axisymmetric notched tensile specimens by using the proposed correction function show good agreement with those from extensometer before diffuse necking and from Bridgman correction at large strain using smooth tensile specimens. Since fracture strain strongly depends on the notch geometry, it is recommended to use axisymmetric notched tensile specimens with smaller a_0/R_0 when applying the proposed correction function to measure material's equivalent stress-strain curve.

Keywords: *equivalent stress-strain curve; low temperature; axisymmetric notched tensile specimen; Bridgman correction; large strain.*

1. Introduction

Identifying material's equivalent stress-strain curve in large strain is very important for large deformation analysis, such as plastic forming [1, 2] and ductile fracture analysis with finite element method [3-8]. Usually, smooth round bar specimens [9, 10] or smooth specimens with rectangular cross-section [11-13] are used to measure material's equivalent stress-strain curves with extensometer. The limitation of such method is that only the data before diffuse necking (different to localized necking) can be used directly. There are several methods to determine material's true stress-strain curve in large range of strain. For thick materials, smooth round bar specimen can be used when the instantaneous minimum cross-section area is measured. The strain ε is then characterized by the specimen minimum cross-section area reduction: $\varepsilon = 2\ln(a_0/a)$, where a_0 and a are the specimen initial and current minimum cross-section radius, respectively. The true stress or axial average stress σ_T is calculated by dividing the load P by the instantaneous minimum cross-section area. For very thin plate material, Zhang [14] proposed a method to calculate the post-necking minimum cross-section area of rectangular cross-section specimens, as a function of specimen thickness reduction. With Zhang's method, true stress-strain curves from flat tensile specimens can be obtained at large strain. It should be noted that after diffuse necking, tri-axial stress state occurs in the necked region. The true stress differs with von Mises equivalent stress σ_{eq} [9, 15], as shown in Fig. 1.

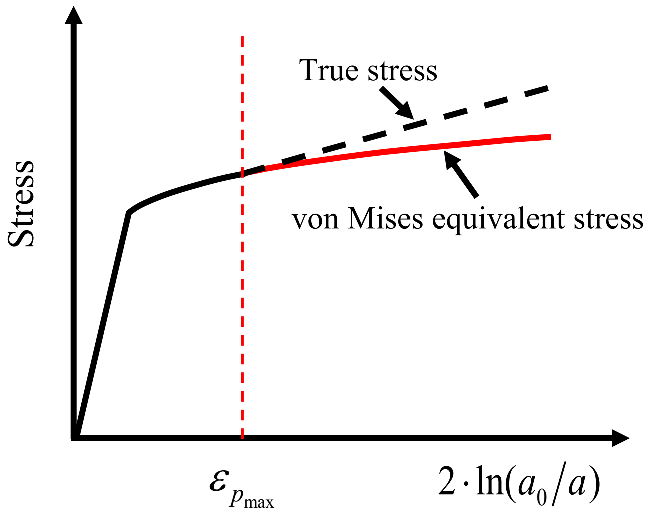

Fig. 1 Illustration of the difference between true stress and von Mises equivalent stress for tensile test with smooth round bar specimen after diffuse necking ($\varepsilon > \varepsilon_{P_{\max}}$).

Diffuse necking occurs after the maximum tensile load, hence the true stress should be corrected when the strain is larger than the strain corresponding to the maximum tensile load, $\varepsilon_{P_{\max}}$. Bridgman [9] performed analytical analysis with necked round bar specimen and proposed a correction factor ξ_B:

$$\begin{aligned} &\xi_B = (1+2R/a)\cdot\ln(1+a/2R) \\ &\sigma_{eq} = \sigma_T/\xi_B \end{aligned} \tag{2}$$

where R is the neck curvature radius. By dividing the true stress in Fig.1 by ξ_B, the material's equivalent stress can be calculated. Indeed, R is very difficult to measure accurately. Le Roy [16] proposed an empirical formula to calculate the notch curvature radius ratio a/R:

$$a/R = 1.1\cdot(\varepsilon - \varepsilon_{P_{\max}}) \tag{3}$$

Combined with Eq. (1) – (2), true stress-strain curve from a smooth round bar specimen can be converted to material's equivalent stress-strain curve after diffuse necking. The Bridgman correction factor ξ_B works well at strain slightly larger than $\varepsilon_{P_{\max}}$. As the strain further increases, errors between the material's equivalent stress and the Bridgman corrected equivalent stress occurs and increases with the increase of strain [15]. The errors range from several percentages to more than 10% [15, 17]. Recent numerical analyses [18-20] show that the stress distribution at the necked specimen minimum cross-section differs significantly with Bridgman's analytical solution. These errors are mainly attributed to the assumption that the equivalent strain is uniform in the specimen minimum cross-section. Similar to the Bridgman method, several other correction methods have been proposed [21]. The main difference of these methods is the determination of the curvature radius of the longitudinal stress trajectories. Though the Bridgman correction method is not very accurate when the strain is large, it still can be used as reference. Ling [22] proposed a so-called weighted average method to measure the true stress-strain curve from rectangular cross-section specimen, by setting the power law hardening as lower bound and the linear hardening as the upper bound for the equivalent stress. The correction proposed by Ling is a kind of hybrid experimental-numerical modeling method and the determination of the weight constant is time consuming. Scheider [23] proposed a correction factor as a function of strain and $\varepsilon_{P_{\max}}$ to derive equivalent stress-strain curve with flat tensile specimen. However, Scheider's method can only be used for specimens with the aspect ratio of 1:4. Choung [24, 25] also proposed a method to measure equivalent stress-strain curves with flat tensile specimens. The minimum cross-section area should be measured manually with digital calipers and a micrometer. It is worth noting that both Scheider [23] and Choung's [24, 25] method are based on inverse numerical analyses.

To measure the true stress-strain curve of each individual material zone in a weldment, Zhang [26] proposed a correction function, with which the true stress-strain curve from an axisymmetric notched tensile specimen can be converted to the corresponding one from a smooth round bar specimen. This method is not accurate at large strain, but lay a foundation for our recent work [27, 28]. With further numerical studies, Tu et al. identified a 'magic' axisymmetric notched tensile specimen [28]. With only one single correction factor, true stress-strain curve from the 'magic' notched specimen can be converted to material's equivalent stress-strain curve in a large range of strain accurately, and no Bridgman correction is needed. The limitation is that failure strain of this 'magic' notched specimen can be much smaller than that from a smooth round bar specimen, sometimes.

Recently, Tu et al. found a new correction function to determine material's equivalent stress-strain curve with 'any' axisymmetric notched tensile specimens [27]. The correction function can be used to the perfectly plastic material and hardening material, and also to weldments. In this study, tensile tests were performed at room temperature, -30 °C and -60 °C with axisymmetric notched tensile specimens machined from a 420 MPa structural steel plates to verify the proposed correction method. The correction function is introduced in detail in section 2. The experimental procedure is presented in section 3. The material's equivalent stress-strain curve were also measured with extensometer and smooth round bar specimens. Before diffuse necking, the equivalent stress-strain curves from axisymmetric notched tensile specimens are compared with those from extensometer. With Eq. (1)-(2), we also performed Bridgman correction with smooth round bar specimen to obtain reference equivalent stress-strain curves after diffuse necking. Results and discussions are presented in section 4. The equivalent stress-strain curves are then verified by numerical analyses in section 5. Main conclusions are presented in section 6.

2. Axisymmetric notched tensile specimen method

Axisymmetric notched tensile specimen has been widely applied in characterizing material's mechanical properties [29-31]. For inhomogeneous material, such as weldment, it is practically impossible to measure the equivalent stress-strain curve in a targeted material zone with cross-weld smooth round bar specimen or flat tensile specimen, due to the nature of practically unpredictable fracture position. By introducing an axisymmetric notch on the smooth round bar specimen, the deformation is restrained mainly in the notched region under uniaxial tensile loading [26-28]. Fig. 2 (a) schematically shows the geometry information of the axisymmetric notched tensile specimen. Similar with smooth round bar specimen, the strain is defined by the minimum cross-section area reduction and the true stress is calculated by dividing load by the current minimum cross-section area:

$$\varepsilon = 2 \cdot \ln\left(a_0/a\right) \tag{4}$$

$$\sigma_T = P/\pi a^2 \tag{5}$$

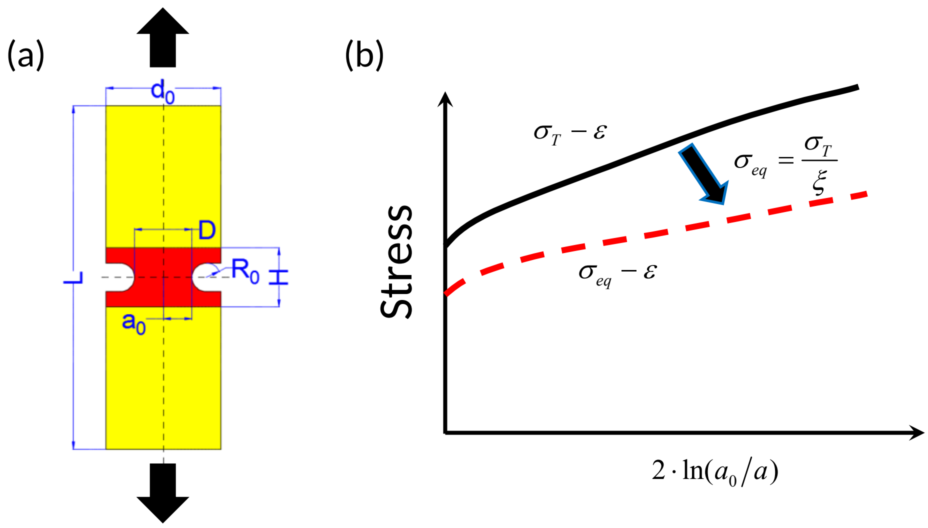

Fig. 2 (a) Geometry of axisymmetric notched tensile specimen. The yellow part can be overmatch, under match or even match with the remain part of the specimen. (b) Conversion of true stress-strain curve from notched specimen to equivalent stress-strain curve by the proposed correction function.

Stress concentration occurs due to the existence of the notch. True stress-strain curve from an axisymmetric notched tensile specimen differs significantly with the material's equivalent stress-strain curve and should be corrected. Our previous study [28] shows that when the specimen geometry requirement $d_0 \geq 3.5a_0$ is fulfilled, true stress-stress curves from axisymmetric notched tensile specimens with the same initial notch radius ratio a_0/R_0 are identical for homogeneous materials. This is true for inhomogeneous material when a_0 is smaller than the material zone length: $a_0 \leq H$.

Recently, we proposed a correction function to convert the true stress-strain curve from any axisymmetric notched tensile specimens to the material's equivalent stress-strain curve [27]. The correction function is written in a general form:

$$\xi = g_{a_0/R_0, n=0}(\varepsilon) \cdot f(\varepsilon_{P_{\max}}) \tag{6}$$

Eq. (5) consists of two parts: the first part describes the notch effect on the true stress-strain curves of the perfectly-plastic material, and displays as a linear function of the true strain ε , Eq. (6). The slope, $b_{1,n=0}$, in Eq. (6) depicts the initial notch geometry effect on the evolution of true stress-strain curve from axisymmetric notched tensile specimen. While the intersection, $b_{2,n=0}$, can be explained as the notch induced stress concentration, sharper notch yields higher stress concentration. The slope and intersection are given in Eq. (7) and Eq. (8) as a function of the initial notch radius ratio, respectively. The second part, as shown in Eq. (9), is a function of $\varepsilon_{P_{\max}}$, describing the effect of strain hardening on the true stress-strain curve of a notched specimen.

$$g_{a_0/R_0, n=0}(\varepsilon) = (b_{1,n=0} \cdot \varepsilon + b_{2,n=0})_{a_0/R_0} \tag{7}$$

$$b_{1,n=0} = 0.03232 \cdot (a_0/R_0)^2 - 0.27 \cdot (a_0/R_0) + 0.3866 \tag{8}$$

$$b_{2,n=0} = -0.04084 \cdot (a_0/R_0)^2 + 0.3557 \cdot (a_0/R_0) + 1.0577 \tag{9}$$

$$f(\varepsilon_{p_{\max}}) = -0.22942 \cdot \varepsilon_{P_{\max}}^2 - 0.36902 \cdot \varepsilon_{P_{\max}} + 1 \tag{10}$$

When ε and $\varepsilon_{P_{\max}}$ are known, the $\sigma_T - \varepsilon$ curve from an axisymmetric notched tensile specimen can be converted to the material's equivalent stress-strain curve by Eq. (10), as demonstrated in Fig. 2 (b). Details about the derivation of this correction function can be referred to ref. [27].

$$\sigma_{eq} = \sigma_T / \xi \tag{11}$$

3. Experiment procedure

To experimentally verify the correction function, we conducted tensile tests with smooth round bar specimens and axisymmetric notched tensile specimens with initial notch radius ratio, a_0/R_0 , ranging from 0.5 to 3. The specimens were machined from 50 *mm* thick plates of a 420 MPa steel, along the rolling direction. The specimen configurations are shown in Fig. 3. Our previous numerical studies provide a conservative geometry requirement for axisymmetric notched tensile specimens: $d_0 \geq 3.5a_0$. d_0 is the specimen outer diameter, as seen in Fig. 2. In this study, $a_0 = 6\ mm$ and $d_0 = 20\ mm$. The specimen outer diameter is 1 mm smaller than the geometry requirement ($d_0 \geq 3.5a_0$). In order to guarantee that the specimen geometry can be used, we simply performed numerical analysis with power-law hardening material and found that the correction function was still valid.

The tests were carried out at room temperature, -30°C, and -60°C using a universal test machine Instron 5985, with the loading cell of 250 kN. A liquid nitrogen-cooled temperature chamber was used to create low temperature environment. The tests were divided into two packages: in the first package we tested smooth round bar specimens with extensometer at each test temperature, to provide reference equivalent stress-strain curves; in the second package, we used a digital high speed camera to record the specimen deformation for axisymmetric notched tensile specimens, as well as for smooth round bar specimens. The specimen minimum cross-section diameter in the second package was identified with a so-called 'edge-tracing' or 'edge-detection' method [32]. For all the tests, the specimen was loaded in displacement control with the crosshead speed of 0.3 mm/minute.

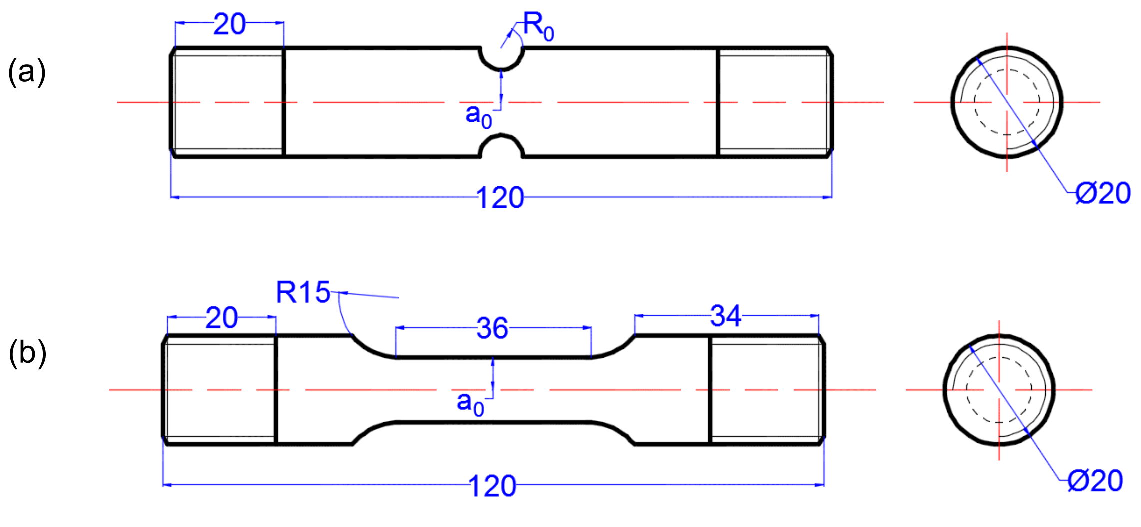

Fig. 3 Sketches of the tensile specimens: (a) axisymmetric notched tensile specimen; (b) smooth round bar specimen.

4. Results and discussion

For the smooth round bar tensile tests with extensometer, the engineering stress σ' is calculated by dividing load by the initial cross-section area ($\sigma' = P/\pi a_0^2$). Engineering strain ε' directly from extensometer and corresponding engineering stress are converted to true strain and true stress by Eq. (11) and Eq. (12):

$$\sigma_T = \sigma'(1+\varepsilon') \tag{12}$$

$$\varepsilon = \ln(1+\varepsilon') \tag{13}$$

Fig. 4 presents the true stress-strain curves at room temperature, -30°C and -60°C. Obvious temperature effect can be found: true stress-strain curve obtained at lower test temperature presents to be higher. It can also be found that the strain corresponding to the onset of diffuse necking ($\varepsilon_{P_{\max}}$, intersections of the dash lines and the horizontal axis) also increases slightly with decreasing testing temperature. Before diffuse necking, the smooth round bar specimen deforms uniformly, true stress-strain curve also represents material's equivalent stress-strain curve. Therefore, true stress-strain curves in Fig. 4 will be used as reference before diffuse necking in the following discussion.

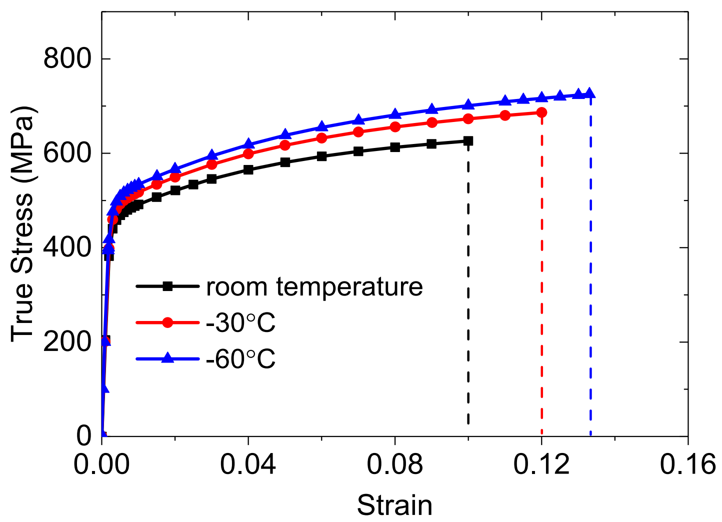

Fig. 4 True stress-strain curves from smooth round bar specimens with extensometer.

For the tensile tests in the second package, the specimen deformation was recorded with a digital high speed camera. The originally circular cross sections almost remained circular just before fracture, as indicated by the minor difference in diameter measurement in the minimum cross-section. The strain for smooth round bar specimens is calculated by Eq. (3), the same for the axisymmetric notched tensile specimens. Engineering stress-strain curves for all the tests in the second package are presented in Fig. 5. As expected, the engineering stress increases with strain firstly; after reaching the maximum value it decreases. Axisymmetric notched tensile specimen with a higher initial notch radius ratio corresponds to a larger peak engineering stress. For example, for the tests performed at room temperature, the maximum engineering stress for specimen with $a_0/R_0 = 0.5$ is 673.55 MPa; while for specimen with $a_0/R_0 = 3$, the maximum engineering stress is 903.11 MPa, $\varepsilon_{P_{\max}}$ is shown with red dash lines in Fig. 5. It can be seen that $\varepsilon_{P_{\max}}$ for smooth round bar specimen and axisymmetric notched tensile specimens is approximately the same at same testing temperature. This result indicates that for this 420 MPa structural steel, $\varepsilon_{P_{\max}}$ is independent of the specimen notch geometry. It can also be observed that $\varepsilon_{P_{\max}}$ for this material is sensitive to temperature, and it increases slightly with decreasing testing temperatures.

True stress for all the tests in the second package are calculated with Eq. (4). Corresponding true stress-strain curves are presented in Fig. 6. For the smooth round bar specimens in the second package, true stress-strain curve before diffuse necking is exactly the material's equivalent stress-strain curve. After diffuse necking, true stress-strain curves of smooth round bar specimens in Fig. 6 are corrected by Bridgman correction: Eq. (1) and Eq. (2). True stress-strain curves for axisymmetric notched tensile specimens in Fig. 6 are then corrected with Eq. (10). Corresponding equivalent stress-strain curves are presented in Fig. 7, together with the true stress-strain curves with extensometer and equivalent stress-strain curves after performing Bridgman correction with smooth round bar specimens in the second package. Very good agreements can be seen in Fig. 7 between the true stress-strain curves from extensometer and equivalent stress-strain curves corrected by Eq. (10) with axisymmetric notched tensile specimens, at each test temperature. After diffuse necking, equivalent stress-strain curves corrected by Eq. (10) with the axisymmetric notched tensile specimens agree well with the Bridgman corrected equivalent stress-strain curve from smooth round bar specimen, when the strain is smaller than 0.528, 0.699, 0.742 for the tests performed at room temperature, -30°C, and -60°C, respectively. After then, slight difference can be found. The equivalent stress corrected by Eq. (10) is slightly lower than those from the Bridgman correction.

For axisymmetric notched tensile specimen with sharper initial notch (larger a_0/R_0), the specimen failed at smaller strain than that with smaller initial notch radius ratio. For example, for the tests conducted at -30°C, the specimen with $a_0/R_0 = 3$ failed when $\varepsilon = 0.525$; while for the specimen with $a_0/R_0 = 0.5$, it failed at the strain $\varepsilon = 1.14$. This can be explained that the strain at fracture is strongly dependent of stress triaxiality T, which is defined by the ratio of hydrostatic stress and von Mises equivalent stress [33-36]. Fracture strain decreases with the increase of stress triaxiality in the range $T \geq 1/3$. For axisymmetric notched tensile specimen, the stress triaxiality is a function of notch radius ratio and larger than 1/3. Larger a_0/R_0 corresponds to a higher stress triaxiality, therefore, resulting in a smaller failure strain. On the purpose of measuring equivalent stress-strain curve with our correction function in large strain, it is therefore not recommended to use specimens with very larger initial notch radius ratio.

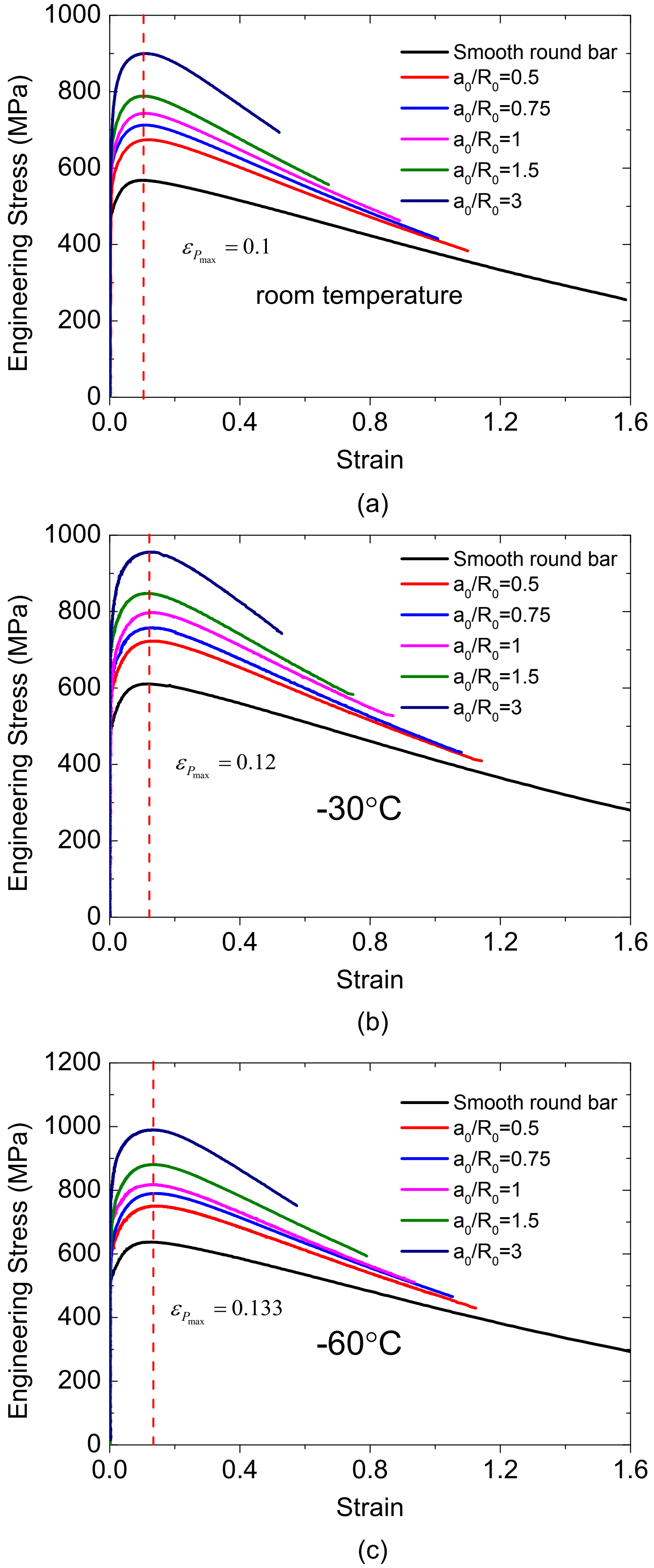

Fig. 5 Engineering stress-strain curves of smooth round bar and axisymmetric notched tensile specimens: (a) room temperature; (b) -30℃; (c) -60℃. $\varepsilon_{p_{\max}}$ *is also shown with red dash lines.*

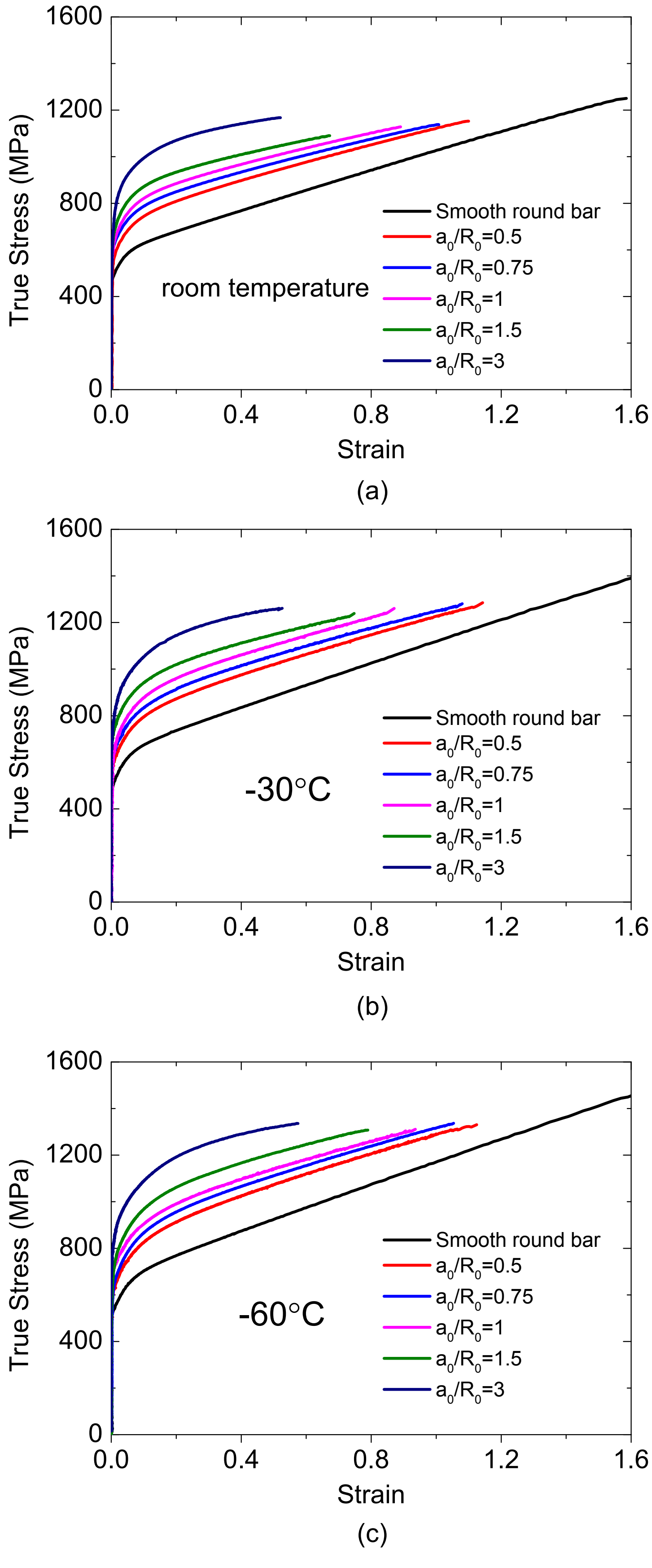

Fig. 6 True stress-strain curves of smooth round bar and axisymmetric notched tensile specimens: (a) room temperature; (b) -30℃; (c) -60℃.

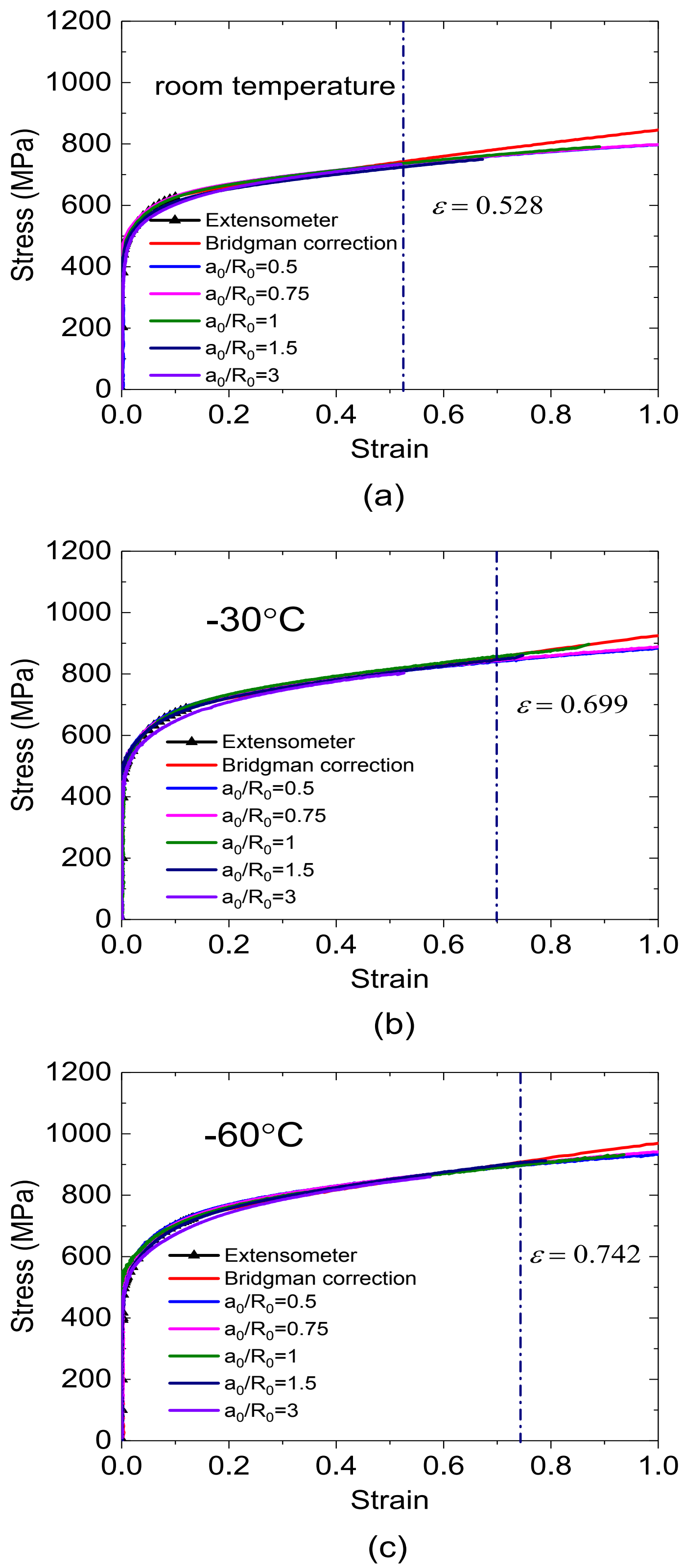

Fig. 7 Equivalent stress-strain curves obtained from axisymmetric notched tensile specimens with the correction function: (a) room temperature; (b) -30°C; (c) -60°C. Equivalent stress-strain curve from smooth round bar specimen from extensometer (before diffuse necking) and from Bridgman correction are also shown for reference.

5. Validation of the equivalent stress-strain curve

The correction method is derived with power-law hardening materials in an inverse manner. Attention should be paid for the application of this correction method, since materials can follow different hardening rules. To guarantee the accuracy of the equivalent stress-strain curve obtained with the correction method, a fast and efficient way is to compare load-strain curves from tests and from numerical analysis, assuming the derived equivalent stress-strain curve as material's equivalent stress-strain curve and used for numerical modeling. Fig. 8 schematically presents the validation procedure. True stress-strain curve from axisymmetric notched tensile specimen in Fig. 8 (a) are corrected with Eq. (10) to obtain the equivalent stress-strain curve in Fig. 8 (b). The equivalent stress-strain curve in Fig. 8 (b) is then used as input stress-strain curve for numerical analysis. Load-strain curves from numerical simulation (see in Fig. 8 (d)) are then compared with those from test, as shown in Fig. 8 (e). When the load-strain curves from test and from numerical simulation show very good agreement, it indicates that the equivalent stress-strain derived with the proposed correction method is accurate.

As an example, equivalent stress-strain curves derived with the axisymmetric notched tensile specimen with $a_0/R_0 = 0.5$ at each test temperature are used for numerical analyses. The geometry used for numerical analyses is the same as in experiments. Numerical analyses were perforemed with Abaqus/Standard 6.14. Axisymmetric model is used with the 4-noded axisymmetric reduced integration element (CAX4R). The element size is approximately 0.4*0.4 mm in the notch region. Larger deformation is accounted. Symmetric boundary condition is applied in the symmetry plane. The specimen is modelled in displacement control, the same as in the expeirment. Load-strain curves from the experiments and from numerical analyses are presented in Fig. 9.

It can be seen that the load-strain curves from numerical analyses present very good agreement with those from experiments, at each test temperature. It indicates that the deformation on the specimen during loading process can be well captured. It also indicates that the equivalent stress-strain curves derived with the correction function are accurate for this 420 MPa structural steel.

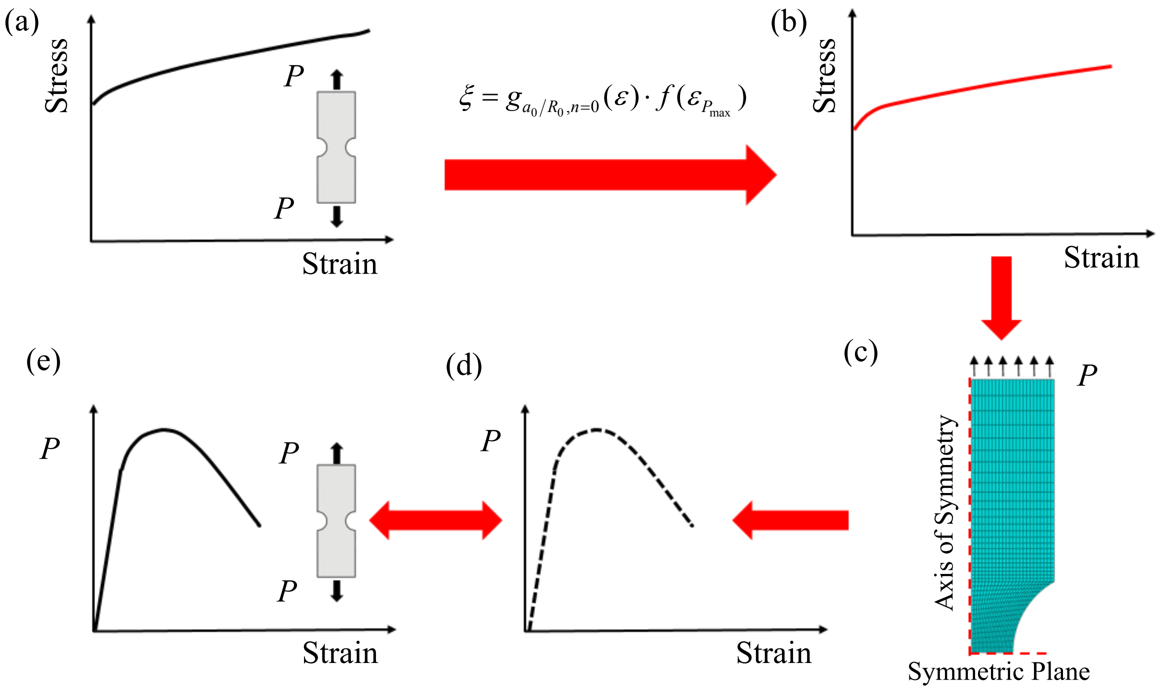

Fig. 8 Procedure for the validation of the equivalent stress-strain curves from axisymmetric notched specimens. (a) true stress-strain curve from axisymmetric notched specimens tensile tests; (b) equivalent stress-strain curve obtained with the proposed correction method; (c) Numerical simulation of tensile tests. (d) Load-strain curves from numerical simulation; (e) Load-strain curves from test.

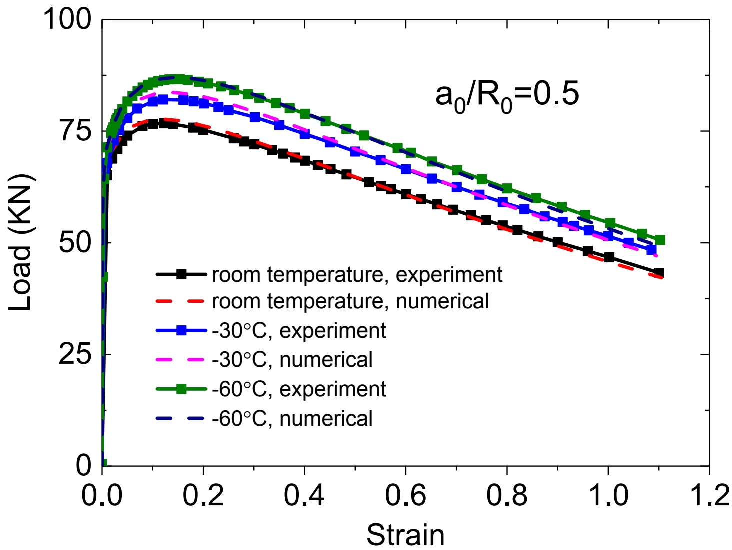

Fig. 9 Comparison of load-strain curves from experiments and from numerical analyses for axisymmetric notched specimen with $a_0/R_0 = 0.5$ *at each test temperature.*

6. Concluding remarks

In this paper, we performed tensile tests with axisymmetric notched tensile specimens with a_0/R_0 ranging from 0.5 to 3 to experimentally verify the recent proposed correction function, by measuring equivalent stress-strain curve of a 420 MPa structural steel at room temperature, -30°C and -60°C, respectively. Equivalent stress-strain curves by converting true-strain curves from axisymmetric notched tensile specimens with the proposed correction function agree very well with true stress-strain curves from smooth round bar specimen with extensometer together with Bridgman correction. Comparing load-strain curves from the experimental tensile tests and those from numerical modeling, it indicates that the proposed correction method works well to explore the material's stress-strain curve. Considering the derivation of this correction function, the authors suggest to use axisymmetric specimens with a_0/R_0 ranging from 0.5 to 3 and the hardening exponent n from 0 to 0.35. It is worth noting that the proposed correction function can also be used to measure the equivalent stress-strain curve of each individual material zone in a weldment, by locating the notch in the targeted material zone, once the specimen geometry requirements ($d_0 \geq 3.5a_0$, $a_0 \leq H$) are fulfilled. Due to the stress triaxiality dependence of fracture strain, it is not suggested to use specimens with very sharp notch (large a_0/R_0) to measure material's equivalent stress-strain curve. For materials display highly anisotropy, this method may not be suitable. We recommend to run numerical analysis to verify the equivalent stress-strain curve derived with the correction function to guarantee the validity of test results.

Acknowledgement

The Chinese Scholarship Council is greatly acknowledged for the financial support. The authors wish to thank the Research Council of Norway for funding through the Petromaks 2 Programme, Contract No.228513/E30.

Reference

[1] F.M. Andrade Pires, J.M.A. César de Sá, L. Costa Sousa, R.M. Natal Jorge, Numerical modelling of ductile plastic damage in bulk metal forming, International Journal of Mechanical Sciences 45(2) (2003) 273-294.

[2] O.M. Badr, F. Barlat, B. Rolfe, M.-G. Lee, P. Hodgson, M. Weiss, Constitutive modelling of high strength titanium alloy Ti-6Al-4 V for sheet forming applications at room temperature, International Journal of Solids and Structures 80 (2016) 334-347.

[3] Z.L. Zhang, M. Hauge, C. Thaulow, Two parameter characterization of the near-tip stress field for a bi-material elastic-plastic interface crack, International Journal of Fracture 79 (1996) 65-83.

[4] E. Østby, C. Thaulow, Z.L. Zhang, Numerical simulations of specimen size and mismatch effects in ductile crack growth – Part I: Tearing resistance and crack growth paths, Engineering Fracture Mechanics 74(11) (2007) 1770-1792.

[5] E. Østby, C. Thaulow, Z.L. Zhang, Numerical simulations of specimen size and mismatch effects in ductile crack growth – Part II: Near-tip stress fields, Engineering Fracture Mechanics 74(11) (2007) 1793-1809.

[6] J. Xu, Z.L. Zhang, E. Østby, B. Nyhus, D.B. Sun, Effects of crack depth and specimen size on ductile crack growth of SENT and SENB specimens for fracture mechanics evaluation of pipeline steels, International Journal of Pressure Vessels and Piping 86(12) (2009) 787-797.

[7] J. Xu, Z.L. Zhang, E. Østby, B. Nyhus, D.B. Sun, Constraint effect on the ductile crack growth resistance of circumferentially cracked pipes, Engineering Fracture Mechanics 77(4) (2010) 671-684.

[8] J. Shuai, S. Tu, J. Wang, X. Ren, J. He, Z. Zhang, Determining critical CTOA from energy-load curves with DWTT specimen, Engineering Fracture Mechanics 186 (2017) 47-58.

[9] P.W. Bridgman, Studies in large plastic flow and fracture, MaGraw-Hill, New York, 1952.

[10] D.J. Celentano, Analysis of the Bridgman procedure to characterize the mechanical behavior of materials in the tensile test experiments and simulation, Journal of Applied Mechanics 72 (2005) 149-152.

[11] W.J. Yuan, Z.L. Zhang, Y.J. Su, L.J. Qiao, W.Y. Chu, Influence of specimen thickness with rectangular cross-section on the tensile properties of structural steels, Materials Science and Engineering: A 532 (2012) 601-605.

[12] Z.L. Zhang, J. Ødegård, O.P. Søvik, Determining true stress-strain curve for isotropic and anisotropic materials with rectangular tensile bars: method and verifications, Computational Materials Science 20 (2001) 77-85.

[13] Z.L. Zhang, J. Ødegård, O.P. Søvik, C. Thaulow, A study on determining true stress–strain curve for anisotropic materials with rectangular tensile bars, International Journal of Solids and Structures 38 (2001) 4489-4505.

[14] Z.L. Zhang, M. Hauge, J. Ødegård, C. Thaulow, Determining material true stress-strain curve from tensile specimens with rectangular cross-section, International Journal of Solids and Structures 36 (1999) 3497-3516.

[15] G. La Rosa, G. Mirone, Risitano. A, Postnecking elastoplastic characterization degree of approximation in the bridgman method and properties of the flow stress true stress ratio, Metallurgical and Materials Transactions A 34 (2003) 615-624.

[16] G.L. Roy, J.D. Embury, G. Edward, M.F. Ashby, A model of ductile fracture based on the nucleation and growth of voids, Acta Metallurgica 29 (1981) 1509-1522.

[17] G. Mirone, A new model for the elastoplastic characterization and the stress–strain determination on the necking section of a tensile specimen, International Journal of Solids and Structures 41(13) (2004) 3545-3564.

[18] Y. Bai, X. Teng, T. Wierzbicki, On the Application of Stress triaxiality formula for plane strain fracture testing, Journal of Engineering Material and Technology 131 (2009).

[19] Y. Bao, Dependence of ductile crack formation in tensile tests on stress triaxiality, stress and strain ratios, Engineering Fracture Mechanics 72(4) (2005) 505-522.

[20] Y. Bao, T. Wierzbicki, On the cut-off value of negative triaxiality for fracture, Engineering Fracture Mechanics 72(7) (2005) 1049-1069.

[21] M. Gromada, G. Mishuris, Andreas, Correction formulae for the stress distribution in round tensile specimens at neck presence, Springer2011.

[22] Y. Ling, Uniaxial true stress-strain after necking, AMP Journal of Technology 5 (1996) 37-48.

[23] I. Scheider, W. Brocks, A. Cornec, Procedure for the determination of true stress-strain curves from tensile tests with rectangular cross-section specimens, Journal of Engineering Material and Technology 126 (2004) 70-76.

[24] J. Choung, Comparative studies of fracture models for marine structural steels, Ocean Engineering 36(15-16) (2009) 1164-1174.

[25] J.M. Choung, S.R. Cho, Study on true stress correction from tensile tests, Journal of Mechanical Science and Technology 22(6) (2008) 1039-1051.

[26] Z.L. Zhang, M. Hauge, C. Thaulow, J. Ødegård, A notched cross weld tensile testing method for determining true stress–strain curves for weldments, Engineering Fracture Mechanics 69 (2002) 353-366.

[27] S. Tu, X. Ren, J. He, Z. Zhang, A method for determining material's equivalent stress-strain curve with any axisymmetric notched tensile specimens without Bridgman correction, International Journal of Mechanical Sciences 135 (2018) 656-667.

[28] S. Tu, X. Ren, B. Nyhus, O.M. Akselsen, J. He, Z. Zhang, A special notched tensile specimen to determine the flow stress-strain curve of hardening materials without applying the Bridgman correction, Engineering Fracture Mechanics 179 (2017) 225-239.

[29] N. Noda, Y. Takase, Stress concentration formula useful for all notch shape in a round bar (comparison between torsion, tension and bending), International Journal of Fatigue 28(2) (2006) 151-163.

[30] F. Berto, P. Gallo, P. Lazzarin, High temperature fatigue tests of un-notched and notched specimens made of 40CrMoV13.9 steel, Materials & Design 63 (2014) 609-619.

[31] A. Wormsen, M. Avice, A. Fjeldstad, L. Reinås, K.A. Macdonald, E. Berg, A.D. Muff, Fatigue testing and analysis of notched specimens with typical subsea design features, International Journal of Fatigue 81 (2015) 275-298.

[32] S. Tu, X. Ren, J. He, Z. Zhang, Study of low temperature effect on the fracture locus of a 420 MPa structural steel with the edge tracing method, Fatigue & Fracture of Engineering Materials & Structures On line (2018).

[33] T. Børvik, O.S. Hopperstad, T. Berstad, On the influence of stress triaxiality and strain rate on the behaviour of a structural steel. Part II. Numerical study, European Journal of Mechanics - A/Solids 22(1) (2003) 15-32.

[34] T. Børvik, O.S. Hopperstad, S. Dey, E.V. Pizzinato, M. Langseth, C. Albertini, Strength and ductility of Weldox 460 E steel at high strain rates, elevated temperatures and various stress triaxialities, Engineering Fracture Mechanics 72(7) (2005) 1071-1087.

[35] O.S. Hopperstad, T. Børvik, M. Langseth, K. Labibes, C. Albertini, On the influence of stress triaxiality and strain rate on the behaviour of a structural steel. Part I. Experiments, European Journal of Mechanics - A/Solids 22(1) (2003) 1-13.

[36] Z.L. Zhang, E. NIEMI, Studies on the ductility predictions by different local failure criteria, Engineering Fracture Mechanics 48 (1994) 529-540.